frontiers | Frontiers in Energy Research

TYPE Original Research
PUBLISHED 12 January 2023
DOI 10.3389/fenrg.2022.1008356

OPEN ACCESS

EDITED BY
Yibo Li,
Southwest Petroleum University, China

REVIEWED BY
Xiong Liu,
Xi'an Shiyou University, China
Yisheng Hu,
Southwest Petroleum University, China

*CORRESPONDENCE
Feng Xu,
xufeng01@cnpcint.com

SPECIALTY SECTION
This article was submitted to Advanced Clean Fuel Technologies, a section of the journal Frontiers in Energy Research

RECEIVED 31 July 2022
ACCEPTED 26 September 2022
PUBLISHED 12 January 2023

CITATION
Nie Z, Xu F, Ouyang J, Li X, Zhang J, Liu S, Han J and Li D (2023), Experimental tests and EDFM method to study gas injection in a fractured granite reservoir.
Front. Energy Res. 10:1008356.
doi: 10.3389/fenrg.2022.1008356

Experimental tests and EDFM method to study gas injection in a fractured granite reservoir

Zhiquan Nie[1], Feng Xu[1,2]*, Jingqi Ouyang[1], Xiangling Li[2], Juntao Zhang[1], Shiliang Liu[3], Jinqiang Han[3] and Da Li[3]

[1]China National Oil and Gas Exploration and Development Company Ltd. (CNODC), Beijing, China, [2]Research Institute of Petroleum Exploration and Development Co Ltd (RIPED) CNPC, Beijing, China, [3]Research Institute of Exploration and Development, Petrochina Yumen Oilfield Company, Jiuquan, China

The development of granite reservoirs with high dip fractures has many difficulties, such as a high decline rate, early water breakthrough, and numerous economic losses. Gas injection is usually used to maintain the formation pressure to increase single well productivity, and could be carried out in fractured reservoirs to enhance oil recovery. When injecting associated gas, it meets the environmental protection requirements of the local government to further eliminate the flare, implementing the concept of green and low-carbon development. In this study, both laboratory tests and reservoir simulation have been done to study the feasibility and the benefit of associated gas injection in the research target. For physical stimulation, it mainly includes experiments such as associated gas injection expansion, slim tube, long core displacement, and relative permeability. Through these experiments, the changes in the recovery factor after depletion development and gas displacement are systematically described and the key controls are revealed for improving the recovery ratio of fractured basement reservoirs. For the simulation part, the embedded discrete fracture model processor combining commercial reservoir simulators is fully integrated into the research. A 3D model with complex natural fractures is built to perform the associated gas injection performance of the fractured granite reservoir. Complex dynamic behaviors of natural fractures can be captured, which can maintain the accuracy of DFNs and keep the efficiency offered by structured gridding. Depletion development and gas injection development strategy are optimized in this research. The result shows that oil recovery by using gas injection is increased by 16.8% compared with depletion development by natural energy.

Abbreviations: IOC; International Oil Companies; NOC, National Oil Companies; NFR, Naturally Fractured Reservoir; DPDK, Dual Porosity Dual Permeability; DFM, Discrete Fracture Model; GOR, Gas Oil Ratio; PV, Pore Volume; PVT, Pressure-Volume-Temperature; MMP, Minimum Miscible Pressure; Swi, Irreducible Water Saturation; Sor, Residual Oil Saturation; So, Oil Saturation; kro/krg/krg, Relative Permeability of Oil/Gas/Water; Sgc, Critical Gas Saturation; EDFM, Embedded Discrete Fracture Model.

KEYWORDS

granite reservoir, associated gas injection, EDFM, natural fractures, depletion development

Introduction

In recent years, the low-carbon transformation has become an inevitable trend for the development of global energy companies (Ma et al., 2018; Vardon et al., 2022). Many IOCs and NOCs actively conduct researches on carbon peaking and carbon neutrality, comprehensively formulating a low-carbon strategic transformation path. Normally, oil companies generate a large amount of associated gas in the process of crude oil development, except for one part used to meet the demand of power generation for field daily production, most of it needs to be processed by direct venting or flare combustion, which not only emits a large amount of carbon dioxide into the air, but also wastes the associated natural gas to a large extent. To implement the concept of green and low-carbon development, and meet the environmental protection requirements of the local government to further eliminate the flare, the associated gas reinjection could be carried out in fractured reservoirs to enhance the oil recovery.

Fractured granite reservoirs were discovered in many countries, such as the United Kingdom, India, Egypt, Venezuela, Vietnam, Libya, China, and so on (Dang et al., 2001; Schechter 2002; Van Nguyen et al., 2016; Song et al., 2020; Delamaide et al., 2022). It is known that natural fractures have a great impact on flow properties, production, and ultimate recovery. Most of these reservoirs had high initial production rates and decline rates in the primary production stage. Usually, water and gas injection in fractured reservoirs were considered effective to maintain the reservoir pressure, as seen in Table 1. However, the presence of fractures would lead to rapid water channeling, and the major part of the oil would be trapped in the low permeability matrix blocks in most granite-NFRs. Compared with water flooding, gas can enter smaller microscopic fractures and pores, increasing the gas sweeping volume, and enhancing the oil recovery. Gas flooding could significantly reduce surface tension. The surface tension of oil and gas in immiscible flooding is also only 16%–25% of the oil-water interfacial tension in waterflooding. It is found that the fracture aperture that gas could enter in the gas flooding is 4–7 times smaller than that in water flooding, about 20 times smaller in some oil fields. What is more, it can make full use of the gravity difference between oil and gas in gas flooding, when gas is injected at the top of the reservoir and oil is recovered at the middle and lower parts of the reservoir.

Naturally fractured granite reservoirs are especially difficult to characterize, model, and simulate because of high static and dynamic heterogeneity (Nelson, 2001; Narr et al., 2006; Lonergan et al., 2007; Dipak, 2012; Peng et al., 2020). Researchers have been studying the behavior of fractured reservoirs to capture the physics of fluid flow in such systems (Warren and Root 1963; Cinco-ley and Samaniego-v 1981; Karimi-Fard and Firoozabadi 2003; Hoteit and Firoozabadi 2006; Zhou et al., 2014). To better understand the effect of fractures, several approaches have been proposed, most of which are grounded based on two classes of models, the dual porosity (or dual continuum) and the discrete fracture models. Each class of models has developed to answer some of the challenges associated with modeling and simulation of fractured reservoirs. In the dual porosity approach, an NFR model is represented by two collocated domains, the fracture domain, and the matrix domain. This method could be used in the reservoirs with densely distributed and highly connected fractures, which is very fast and efficient in computation time and has been successfully used in many real NFRs studies. However, there are many simplifications in the models, so they are not suitable for accurately simulating reservoirs with complex and large-scale fractures and fluids flowing along the fractures. In some fractured reservoirs, the fractures do not establish a

TABLE 1 Summary of fractured granite reservoirs.

No.	Reservoir	Country	Lithology	Reservoir Fluid	Development mode
1	Clair field	United Kingdom	Granite	Oil	Water injection
2	Dragon field	Vietnam	Granite	Oil	Water injection
3	La paz field	Venezuela	Limestone, granite	Oil	Water injection
4	Mara field	Venezuela	Granite and metamorphic	Oil	Water injection
5	Nafoora-Augila field	Libya	Granite	Oil	Water injection
6	PY-1 field	India	Weathered granite	Gas &Condensate	Natural energy
7	Shaim field	Russia	Granite and gneiss	Oil	Water injection
8	Sumatra-Beruk Northeast	Indonesia	Metaquartzites, weathered granite	Oil and gas	Natural energy
9	White Tiger field	Vietnam	Granite	Oil and gas	Water/Gas injection
10	Xinglongtai field	China	Metamorphosed granite	Oil and gas	Water/Gas injection
11	Zeit Bay field	Egypt	Fractured Granite	Oil	Gas injection

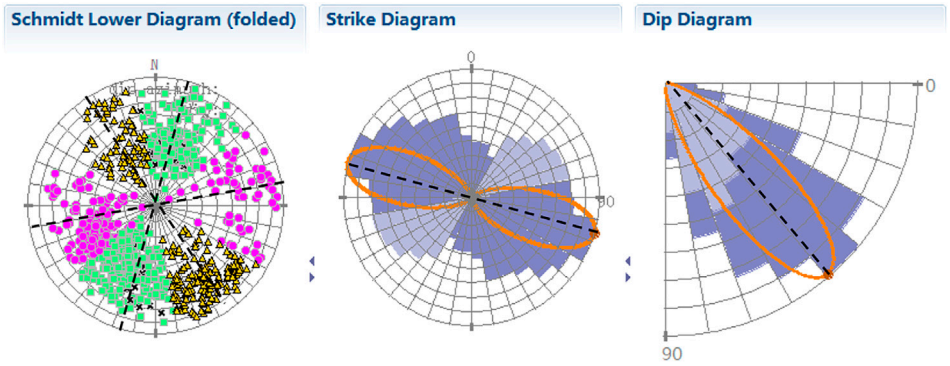

FIGURE 1
Global fracture analysis result.

connected network and thus the continuum assumption is no longer valid. Also, when fracture length is comparable to the size of the computational grid, upscaling and averaging the fracture's properties alter the realistic representation of the network (Long et al., 1982; Long and Witherspoon, 1985). To further eliminate such drawbacks in simulating fractured reservoirs, a new kind of model, called the Discrete Fracture Model (DFM), was proposed. In DFMs, each fracture is modeled explicitly through the application of unstructured gridding. Complex fracture geometry can be mostly represented by using this approach, and large quantities of small-scale grids are generated around the fractures. However, the DFM models have complicated gridding and time-consuming computation, so the models have great limitations in real field reservoir simulation. To solve the strait above, a 2D embedded discrete fracture model (EDFM) was proposed to keep the accuracy of DFMs while holding the efficiency presented by structured gridding (Lee et al., 2001; Li and Lee 2008; Hajibeygi et al., 2011). Last few years, many scholars spread the EDFM for 3D reservoir simulators (Moinfar et al., 2014; Cavalcante Filho et al., 2015; Xu et al., 2017, Xu F et al., 2018), making the EDFM method more useful in the fractured reservoirs.

In this study, both Lab tests and reservoir simulation have been done to study the feasibility and the benefit of associated gas injection in the research target. For physical stimulation, it mainly includes experiments such as associated gas injection expansion, slim tube, long core displacement, and relative permeability. Through these experiments, the changes in the recovery factor after water flooding and gas displacement are systematically described and the key controls are revealed for improving the recovery ratio of fractured basement reservoirs. For the simulation part, the EDFM processor combining commercial reservoir simulators is fully integrated into the research. A 3D model with complex natural fractures is built to perform the associated gas injection performance of the fractured granite reservoir.

TABLE 2 Composition of the associated gas.

Component	Composition, mol%
CO_2	0.3
N_2	5.7
C_1	62.2
C_2	11.0
C_3	13.0
iC_4	3.6
nC_4	2.9
iC_5	0.4
nC_5	0.2
C_{6+}	0.7

Reservoir characteristics

The research area is a brand-new oil field, the natural fractures play a major role in oil production for this specific granite reservoir. The reservoir thickness is about 150 m and could be separated into three layers vertically. The reservoir is composed of complex lithologies, which include metamorphic rocks and magmatic rocks. The structure characteristic of this reservoir is complicated by a basement fault system and long exposure history, complex natural fractures and vugs are well developed. The basement reservoir is characterized by low porosity and low permeability. Generally, the porosity is 2%–6%, and permeability is less than 10 mD. It is impossible to produce commercially without fracture communication. Fracture orientations are organized into three sets of fractures. One major trend (WNW-ESE), one secondary trend (ENE-WSW), and one minor trend (NS) are recognizable. Figure 1 shows the stereo plot of the 807 fractures interpreted in the reservoir units of the wells considered for the analysis. For each of the three sets of fractures, the average dip angle is computed

TABLE 3 Displacement efficiency at different pressures (96.8°C).

Pressure (MPa)	Displacement efficiency (%)
12.5	57.57
16	75.14
18	88.18
20	90.48
25	92.38

using the entire population of diffuse fractures and fracture clusters from all of the wells, ranging from 60° to 85°.

The wells completed in the area have high oil production, low water production, and low gas oil ratio (GOR). The effective fracture permeability interpreted based on the well testing method ranges from 118 to 3,410 mD, which revealed strong heterogeneity in the reservoir. Although the average well space is as far as 800 m, well interference between some wells is detected.

Experimental tests

The oil sample used in the experiment is from a typical well in the fractured granite reservoir, which belongs to a black oil system with low methane, low hydrocarbon intermediates, and high heavy hydrocarbon. The content of C_1+N_2 accounts for 9.56%, the content of C_2 ~ C6 + CO2 14.145%, and the content of C7+ 76.29%. The associated gas used in the experiment is from a high gas rate well in the main oilfield, with C1 + N2 accounting for 67.9%, C2 ~ C_6 + CO_2 32.1%, which is a rich gas with high methane content, as seen in Table 2. The formation temperature is 96.8°C the formation pressure is 12.3 MPa, and the gas/oil ratio is 15.9 m^3/m^3.

Phase behavior experiment

The gas/oil ratio is low, so the crude oil is under-saturated. The saturation pressure measured by the flash experiment is 2.55 MPa. The difference between the formation pressure and the bubble point pressure is so large that the elastic energy is weak, and therefore, it is necessary to inject water or gas to increase formation energy and produce the reservoir. Figure 2.

The P-V relationship curve shows that the increase of the gas-liquid relative volume is not significant after the crude oil is degassed. Affected by the low gas/oil ratio and under-saturation state, the PVT properties of the formation oil have minor changes during the process of multistage degassing while the formation pressure decreases due to the production.

The effects of injecting associated gas on increasing the dissolved gas volume in the crude oil and the expansion of the crude oil are studied. Multiple parameters are analyzed to determine the flow mechanism of associated gas in the fractured granite reservoir, such as the gas/oil ratio, saturation pressure, expansion factor, saturated oil density, viscosity, and shrinkage ratio.

The slim tube experiment is the main experimental method to determine the minimum miscible pressure (MMP) of a given injected gas. Related terms mainly refer to multiple-contact miscibility and MMP. Based on the measured data under experimental pressures, displacement efficiency to displacement pressures for all slim tube experiments at 1.2 PV of associated gas was plotted, and a linear correlation was fitted to the data. The MMP was predicted according to the fitted correlation. The results showed that when the injection pressure of associated gas was 18.45 MPa, the displacement efficiency at 1.2 PVs was able to be more than 90%, that is to say, 18.45 MPa could be regarded as the MMP, and when the pressure was higher, the characteristics of miscible flooding could appear (Table 3).

When the gas was injected at the formation pressure (12.3 MPa), the results of the back multiple-contact displacement experiment showed that the displacement process followed the mechanism of multiple-contact condensation gas displacement, and the injection of the associated gas at the original formation pressure is multiple-contact condensation near-miscible flooding. Figure 3.

When the pressure was increased to 16.9 MPa, the associated gas injection was able to achieve multiple-contact condensation miscible displacement. Figure 4.

TABLE 4 PVT data of injecting different volumes of the associated gas (96.8°C).

Gas injection rate, mol%	GOR, m3/m3	Expansion Coefficient	Bubble point Pressure, MPa	Surface oil density, g/cm^3	Saturated oil density, g/cm^3	Saturated oil viscosity, mPa·s
0	16.0	1.0000	2.5	0.8036	0.7216	8.8681
10	29.1	1.0350	4.0	0.8039	0.7069	6.2536
20	43.2	1.0800	5.6	0.8041	0.6898	4.1419
30	61.4	1.1370	7.3	0.8042	0.6695	2.6495
40	85.6	1.2150	9.2	0.8042	0.6449	1.5673
50	119.5	1.3260	11.2	0.8042	0.6146	0.8636
60	170.6	1.4950	13.4	0.8042	0.5761	0.4445

TABLE 5 Design for relative permeability experiments.

Type	No.	Porosity, %	Permeability, mD	Experiment Design
Matrix core	1	7.01	1.490	Gas/water flooding
	2	5.24	0.362	Gas/water flooding
	3	2.35	0.288	Gas/water flooding
Cores with Artificial Fractures	4	5.41	51.48	Gas/water flooding
	5	4.55	109.71	Gas/water flooding
	6	5.06	140.65	Gas/water flooding

TABLE 6 Statistics of characteristic values of oil/gas relative permeability curves of matrix cores and cores with artificial fractures.

Type	Core No.	Porosity %	Permeability, mD	Irreducible Water Saturation (S_{wi}) %	Residual Oil Saturation (S_{or}) %	S_o at which $k_{ro} = k_{rg}$	Two phage Flow Range (1- S_{gc}-S_{or}) %	Gas Flooding Efficiency %
Matrix Cores	1	7.01	1.490	33.18	30.93	56.70	35.89	53.71
	2	5.24	0.362	34.44	30.26	61.50	35.30	53.84
	3	2.35	0.288	34.35	27.31	54.40	38.34	58.40
	Total	4.87	0.713	33.99	29.50	57.53	36.51	55.32
Cores with Artificial Fractures	4	5.41	51.48	34.35	32.83	54.60	32.82	49.99
	5	4.55	109.71	32.4	24.32	61.50	43.28	64.02
	6	5.06	140.65	34.7	26.9	58.20	38.40	58.81
	Total	5.01	100.61	33.82	28.02	58.10	38.17	57.61

The expansion experiments of injecting associated gas were conducted at the formation temperature of 96.8°C in (Table 4). The results showed that gas injection had a good effect on increasing the dissolved gas volume in the crude oil and the expansion of the crude oil. The effects of different injected mediums and injected volumes were compared through experiments. It was proved that the associated gas had a good performance.

After the associated gas was injected into the reservoir oil, the saturation pressure of crude oil increased, and the greater the gas injection volume, the greater the saturation pressure, and the magnitude of the increase rose with the gas injection rate. Under the original formation pressure, the increased dissolved gas volume of associated gas injection was about 57% mol.

The expansion coefficients of crude oil and gas-oil ratios both increased with the gas injection rate because gas has certain solubility in crude oil and could expand the crude oil. For associated gas injection, the viscosity of crude oil at saturation pressure decreased significantly, and the viscosity of crude oil at saturation pressure decreased rapidly first and then slowly. However, the density of reservoir oil displayed first a slow and then a fast-decreasing trend.

The wax precipitation conditions were analyzed in the process of gas injection for the fractured basement reservoir. From the P-T phase diagram, the trajectory of the solid precipitation was close to a vertical line that decreased with pressure, and the solid phase precipitation temperatures of the oil were between 14 °C and 28 °C. What's more, the improved equation of state PR was used to calculate the wax precipitation for the composition distribution of the formation fluids in the NFR. The calculation pressure started with the formation pressure, and then the pressure was reduced successively, and the wax and other solids appearance temperature had little change, which was between 17 °C and 19°C, and the wax precipitation temperature was 18.6°C. Based on the P-T phase diagram and improved PR state equation, it is concluded that at the formation temperature (96.8°C) and pressure, the injection of associated gas into the reservoir will not cause wax solid precipitation in the formation. However, wax solid precipitation would occur in the wellbore, so it is needed to consider wax removal measures.

TABLE 7 Statistics of characteristic values of oil/water relative permeability curves of matrix cores and cores with artificial fractures.

Type	Core No.	Porosity %	Permeability, mD	Irreducible Water Saturation (S_{wi}) %	Residual Oil Saturation (S_{or}) %	S_w at which $k_{ro} = k_{rw}$	Two phage Flow Range (1- S_{wi}- S_{or}) %	Water Flooding Efficiency %
Matrix Cores	1	7.01	1.490	33.18	24.43	52.60	42.39	63.44
	2	5.24	0.36	34.08	29.35	48.30	36.57	55.48
	3	2.35	0.29	34.44	25.56	52.20	40.00	61.02
	Total	4.87	0.71	33.90	26.45	51.03	39.65	59.95
Cores with Artificial Fractures	4	5.41	51.48	34.35	32.75	52.20	32.90	50.11
	5	4.55	109.71	32.40	33.46	50.50	34.14	50.5
	6	5.06	140.65	34.70	28.95	52.20	36.35	55.66
	Total	5.01	100.61	33.82	31.72	51.63	34.46	52.09

TABLE 8 A summary of displacement efficiency for different injection methods.

Displacement method	Depletion drive (%)	Displacement at 7.7 MPa(%)	Displacement with shut-in (%)	Displacement efficiency (%)
Associated gas flooding	6.50	60.60	5.75	66.40
Water flooding	5.82	55.72	2.83	58.55

TABLE 9 Basic reservoir and fracture properties used for fractured reservoir simulations.

Parameter	Value
Model dimension (x×y×z)	1200 m × 1200 m × 90 m
Number of gridblocks (DX×DY×DZ)	100 × 100 × 10
Reservoir temperature	96.8 °C
Reservoir permeability	8 mD
Matrix porosity	6%
Rock compressibility	14.5×10^{-4} MPa^{-1}
Initial formation pressure	12.3 MPa
Reservoir mid-depth	1270 m
Reservoir GOR	15.9 m^3/m^3
K_v/K_H	0.10
Well radius	0.15 m
Fracture length	30–90 m
Dip angle	60°–85°
Fracture conductivity	30 mD·m

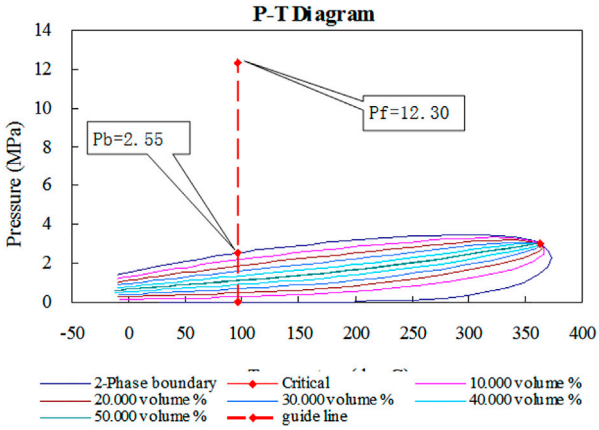

FIGURE 2
P-T Phase behavior of the flash experiment.

Relative permeability experiments

A standard testing workflow of the relative permeability of two-phase fluid (oil and gas) in rock is used to test the relative permeability curve of oil/gas in an unsteady status in gas flooding. The experimental process is that firstly the target rock sample is 100% saturated with water, then displaced water with oil to establish the irreducible water saturation, and in the following gas is used to drive oil to establish the residual oil saturation, the experimental data of oil/gas relative permeability and oil/gas relative permeability curve of each core in the process of gas flooding are determined and normalized.

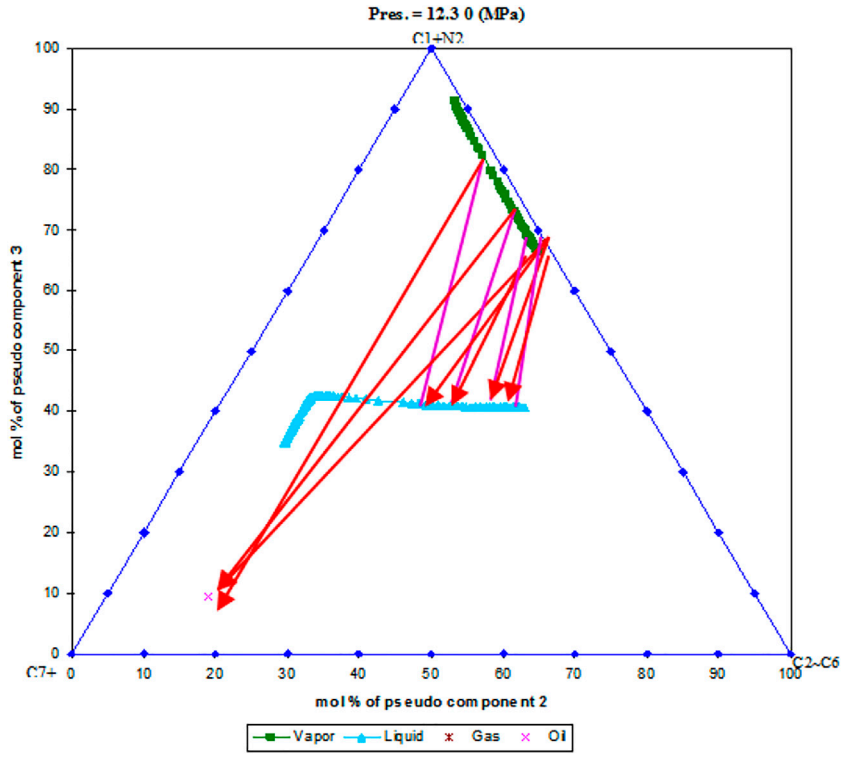

FIGURE 3
Triangle diagram of front multiple contact immiscible displacement of injecting associated gas (12.3 MPa).

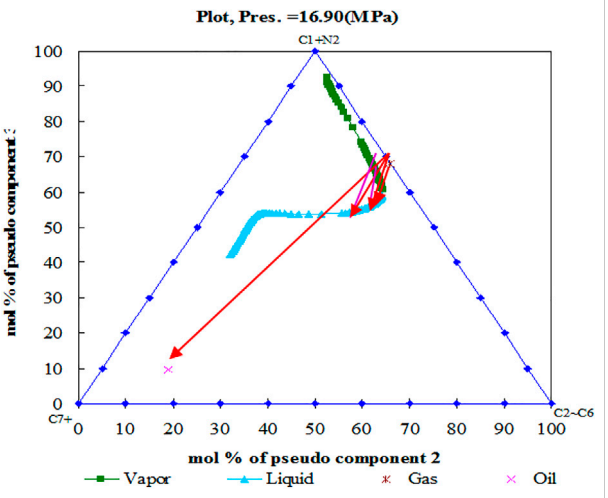

FIGURE 4
Triangle diagram of back multiple-contact immiscible displacement of injecting the associated gas (16.9 MPa).

The relative permeability experimental conditions in the process of gas flooding are: Temperature: 20 °C, Confining pressure: 15MPa, Displacement pressure: 12.3 MPa, Mineralization degree of saturated water: 1460 mg/L, Viscosity of injected gas/water: 0.021/1.03 mPa s, and the formulated oil for displacement with the viscosity of 3.85 mPa s.

In total, there are six relative permeability experiments for six cores divided into two groups, including three groups of gas/water flooding relative permeability experiments for matrix cores, and three groups of gas/water flooding relative permeability experiments for cores with artificial fractures (Table 5).

The relative permeability curve of oil/gas in the matrix core is as follows: the oil/gas flowing zone ranges from 35.3% to 38.34%, and the average two-phase flow range is about 36.51%. The average irreducible water saturation is about 33.99%, and the average residual oil saturation is about 29.5%. The irreducible water saturation at the intersection of the curve is about 57.53%, and the gas flooding efficiency of the rock is about 55.32%. The oil/gas relative permeability curve of cores with artificial fractures is as follows: the oil/gas flowing zone ranges from 32.82% to 43.28%, and the average two-phase flow range is about 38.17%, which is relatively wider. The average irreducible water saturation is about 33.82%, and the average residual oil saturation is about 28.02%. The irreducible water saturation at the intersection

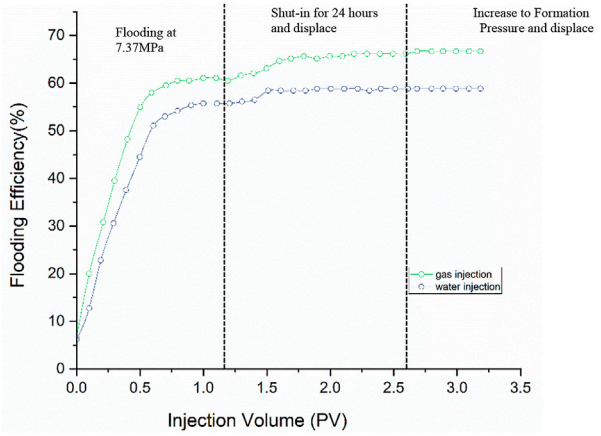

FIGURE 5
Injection PV vs oil flooding efficiency curve.

of the curve is about 58.1%, and the gas flooding efficiency of the rock is about 57.61% (Table 6).

Oil/water relative permeability curves of matrix and cores with artificial fractures are also tested. The characteristics are as follows: the irreducible water saturation of matrix core is higher (33.90%), and the residual oil saturation of matrix core is from 24.43% to 29.35% (26.45% on average), which is lower than that of cores with artificial fractures (31.72%). The range of two-phase (oil/water) flow of matrix core is 36.57%–42.39%, which is higher than 32.90%–36.35% of cores with artificial fractures. The oil recovery efficiency in the matrix core is 59.95% in water flooding, which is higher than that of the matrix core (52.09%) in gas flooding, because the water viscosity is higher than the gas viscosity. However, for the cores with artificial fractures, the efficiency of water flooding is about52.09%, which is lower than that of water flooding at 57.61% (Table 7).

Based on the above, oil/water relative permeability data and curves show that the water flooding efficiency of the matrix core is better than that of the fractured core. The main reason is that the injected water in the process of water flooding quickly broke through along the fractures, resulting in reduced swept area and eventually reduced oil recovery efficiency of cores with artificial fractures. What's more, the test results of the oil/gas relative permeability curve show that more gas can be diffused into more micro pores after cores with artificial fractures, and at the same time the surface tension between the oil and gas is reduced, resulting in a larger swept range, and the final oil recovery efficiency is higher.

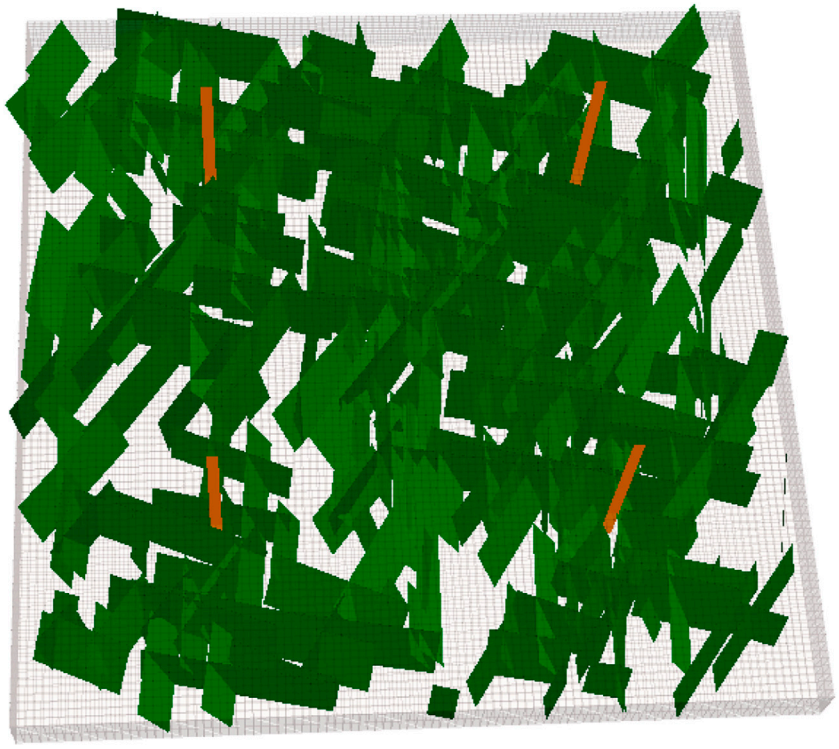

FIGURE 6
NFR simulation model with three sets of fractures.

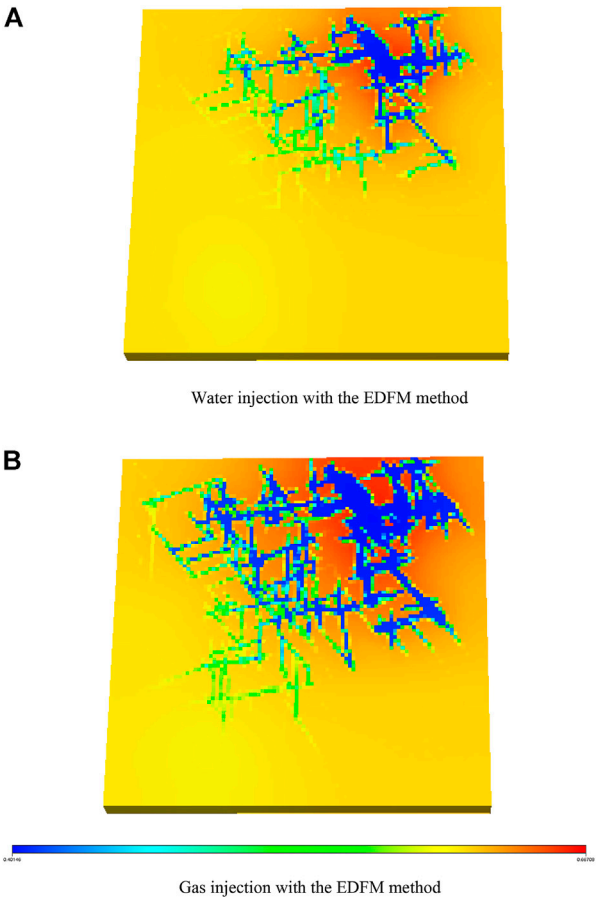

FIGURE 7
Comparison of oil saturation distribution map for water injection and gas injection **(A)** Water injection with the EDFM method **(B)** Gas injection with the EDFM method.

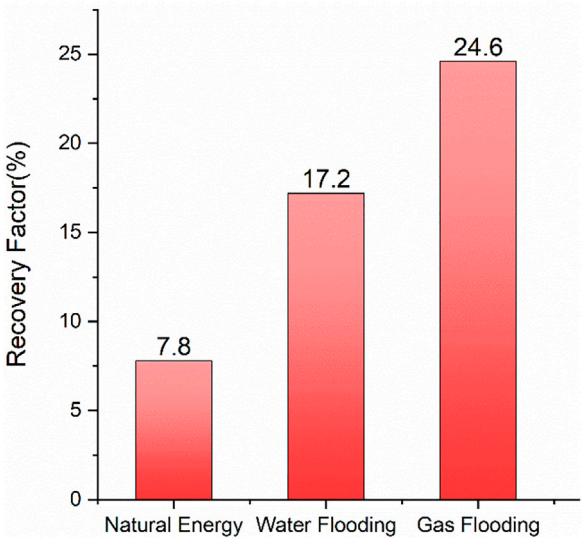

FIGURE 8
Comparison of oil recovery rate with different development mode.

Long core flooding tests

Through the long core displacement method, experimental research was carried out on the displacement efficiency, gas breakthrough, and regulations of gas displacement for the matrix and fractured cores by water/gas injection, and the influence was determined by gas flooding on displacement efficiency at the current reservoir pressure, which provided guidance and reference for the research on displacement mechanism and design of the future gas displacement development.

Water flooding and associated gas flooding were conducted, and it can be seen that (Table 8): 1) water flooding: When the system was produced at the experimental temperature of 96.8 °C from the original formation pressure of 12.3MPa–7.7 MPa by depletion drive, the recovery factor during the depletion process was 5.82%. Subsequently, water was injected until no more oil could be produced, and the displacement efficiency reached 55.72%. Under the current formation pressure, the system was displaced after 24 h of shut-in until no more oil was produced, and the displacement efficiency reached 58.43%. When the pressure was raised to the original formation pressure of 12.3 MPa, the system was displaced after 24-h of shut-in and the ultimate displacement efficiency was 58.55%. By comparing the results before and after shut-in, displacement efficiency was increased by 2.83%. The displacement efficiency with shut-in was improved to a limited extent, and the displacement efficiency with the high-pressure shut-in stage could be increased by 2%, which indicated that the diffusion dialysis ability of water was limited, and there was a little mass exchange with oil in the process of shut-in.

2) Associated gas flooding: With the same experimental process, the reserve recovery by depletion production in this experiment was 6.50%, and the displacement efficiency at the current formation pressure was 60.6%. Shut in for 24 h, the displacement efficiency at the current formation pressure was 65.8%. Shut in for 24 h, the ultimate displacement efficiency under the original formation pressure was 66.4%. Displacement efficiency was increased by 5.75% by shut-in. Figure 5.

Associated gas flooding has better displacement effects than water flooding, because the associated gas is lighter, which moves towards the upper part of the reservoir and causes gravity drainage and it is easy for the associated gas to dissolve in the oil, which would result in continuous mass transfer at the oil/gas contact, delay the breakthrough time and improve displacement efficiency. Shut-in can more intuitively

reflect the difference between gas and water injection because gas has much better diffusion ability while water has seepage ability. In the process of shut-in, the mass transfer between injected gas and oil is much larger, therefore shut-in well in the gas injection process has a much better effect and higher ultimate displacement efficiency.

Reservoir simulation using the EDFM method

To perform the associated gas injection performance of the fractured granite reservoir, a 3D reservoir model with complex natural fractures is built in a numerical-reservoir simulator. The dimensions of NFR are 4,000 ft × 4,000 ft×300 ft, and DX-DY-DZ is 100 × 100×10 in the matrix grid. Reservoir and fracture properties used in the simulation are summarized in Table 9. The relative permeability curve and other parameters are from the Relative Permeability Experiments above. Three sets of natural fractures are randomly generated with different orientations which are put into the NFR. Fracture orientations come from Borehole Imaging (BHI) logging, Set one is the major fracture (WNW-ESE), Set two is the secondary fracture (ENE-WSW), and Set three is the minor fracture (NS). The length of natural fractures ranges from 100 to 300 ft. Each set has about 100 fractures individually, which are randomly distributed in the fractured reservoir. The dip angle ranges from 60° to 80°. The fracture conductivity is 100 md ft from the well testing data.

A novel EDFM processor combining commercial reservoir simulators is fully integrated into the research. EDFM is a non-intrusive method, the calculations of the connection factors, including the NNC transmissibility factor and fracture well index, depend only on the gridding, reservoir permeability, and fracture geometries. Taking the reservoir and gridding parameters as inputs, the EDFM preprocessor provides information such as the number of extra grids, the equivalent properties of these grids, and the NNC pairs to help users make changes in the simulation input. Details of the calculations are discussed in many papers (Xu et al., 2019) Figure 6.

In this modeling method, firstly we have the EDFM model built (shown in Figure 6). EDFM is more accurate for fractured reservoir simulation, since it considers more about the big fractures' impact on fluid flow. All the three sets of fractures (WNW-ESE, ENE-WSW and NS) are used in the simulation model. Considering the fractured reservoir characteristics, four vertical wells are located in the dense fracture area, and producers are completed as open-hole about 180 feet as shown in Figure 6. The simulation time is about 20 years.

Use numerical simulation with EDFM methods to optimize and compare the following two development methods: 1) Natural energy development: three new wells and use natural energy for oil production; 2) Gas injection: Make full use of the difference between oil and gas gravity to inject gas into the reservoir to quickly supplement formation energy and improve the ratio of the total oil produced to OOIP under the condition of overall production from matrix and fracture system.

When the NFR is developed by natural energy, the recovery factor of depletion is about 7.8% after 20 years. In Figure 7, the production performance of water injection and gas injection is observed. Water flooding has a smaller flooding area, and gas flooding has a larger flooding area. Compared with the above two schemes, the recovery factor of water flooding is lower, about 17.2%. The numerical simulation predicts that the recovery factor of associated gas injection is 24.6%, shown in Figure 8. It is seen that associated gas can enter smaller microscopic fractures and pores, increasing the gas sweeping volume, and enhancing the oil recovery. Therefore, the development mode of gas injection is recommended.

Conclusion

1) Associated gas flooding has better displacement performance. Associated gas development has a higher recovery ratio than N_2 because the associated gas is lighter, which moves towards the upper part of the reservoir and causes gravity drainage and because it is easy for the associated gas to dissolve in the oil, which would result in continuous mass transfer at the oil/gas contact, delay the breakthrough time and improve displacement efficiency.
2) The tests of the oil/gas relative permeability curve show that more gas can be diffused into more micro pores after cores with artificial fractures, resulting in a larger swept range, and the final oil recovery efficiency is higher.
3) Compared with natural energy development and associated gas injection, the recovery factor of associated gas flooding is 24.6%, about 16.8% higher than that of depletion development. So the development mode of associated gas injection is recommended in the fractured granite reservoir.

Data availability statement

The original contributions presented in the study are included in the article/supplementary material further inquiries can be directed to the corresponding author.

Author contributions

FX, NZ, and JQ contributed to conception and design of the study. FX organized the database. XL performed the statistical analysis. FX wrote the first draft of the manuscript. JZ, SL, JH, and DL wrote sections of the manuscript. All contributed to

manuscript revision, read, and approved the submitted authors version.

Acknowledgments

The authors would like to acknowledge support from China National Oil and Gas Exploration and Development Company Ltd.

Conflict of interest

Authors FX, NZ, JO, and JZ were employed by the China National Oil and Gas Exploration and Development Company Ltd. (CNODC); Author XL was employed by the Research Institute of Petroleum Exploration and Development Co Ltd (RIPED) CNPC; Authors SL, JH, and DL were employed by the Research Institute of Exploration and Development, Petrochina Yumen Oilfield Company.

The remaining authors declare that the research was conducted in the absence of any commercial or financial relationships that could be construed as a potential conflict of interest.

Publisher's note

All claims expressed in this article are solely those of the authors and do not necessarily represent those of their affiliated organizations, or those of the publisher, the editors and the reviewers. Any product that may be evaluated in this article, or claim that may be made by its manufacturer, is not guaranteed or endorsed by the publisher.

References

Cavalcante Filho, J. S. D. A., Xu, Y., and Sepehrnoori, K. "Modeling fishbones using the embedded discrete fracture model formulation: Sensitivity analysis and history matching," in Proceedings of the Paper SPE 175124 presented at the SPE Annual Technical Conference and Exhibition, Houston, Texas, September 2015, 28–30.

Cinco, L. H., Samaniego, V. F., and Dominguez, A. N. (1978). Transient pressure behavior for a well with a finite-conductivity vertical fracture. *Soc. Petroleum Eng. J.* 18 (04), 253–264. doi:10.2118/6014-pa

Dang, C. T. Q., Chen, Z. J., Nguyen, N. T. B., Bae, W., and Phung, T. H. (2011). Lessons learned and experiences gained in developing the waterflooding concept of a fractured basement-granite reservoir: A 20-year Case study. *J. Can. Petroleum Technol.* 50 (09), 10–23. doi:10.2118/137561-pa

Delamaide, E., Batôt, G., Alshaqsi, A., Alkindy, A., and Al-Mejni, R. "Enhanced oil recovery in naturally fractured reservoirs: State of the art and future perspectives," in Proceedings of the Paper SPE 200076 presented at the SPE Conference at Oman Petroleum & Energy Show, Muscat, Oman, March 2022, 21–23.

Dipak, S. R., Adnan, A., Naveen, K., Saad, M., Laurent, G., De Joussineau, G., et al. (2012). Characterizing and modeling natural fracture networks in a tight carbonate reservoir in the Middle East: A methodology. *Bull. Geol. Soc. Malays.* 58 (3), 29–35. doi:10.7186/bgsm58201205

Hajibeygi, H., Karvounis, D., and Jenny, P. (2011). A hierarchical fracture model for the iterative multiscale finite volume method. *J. Comput. Phys.* 230 (24), 8729–8743. doi:10.1016/j.jcp.2011.08.021

Hoteit, H., and Firoozabadi, A. (2005). Multicomponent fluid flow by discontinuous Galerkin and mixed methods in unfractured and fractured media. *Water Resour. Res.* 41 (11), 1–15. doi:10.1029/2005wr004339

Karimi-Fard, M., and Firoozabadi, A. (2003). Numerical simulation of water injection in fractured media using the discrete-fracture model and the galerkin method. *SPE Reserv. Eval. Eng.* 6 (02), 117–126. doi:10.2118/83633-pa

Lee, S. H., Lough, M. F., and Jensen, C. L. (2001). Hierarchical modeling of flow in naturally fractured formations with multiple length scales. *Water Resour. Res.* 37 (3), 443–455. doi:10.1029/2000wr900340

Li, L., and Lee, S. H. (2008). Efficient field-scale simulation of black oil in a naturally fractured reservoir through discrete fracture networks and homogenized media. *SPE Reserv. Eval. Eng.* 11 (04), 750–758. doi:10.2118/103901-pa

Lonergan, L., Jolly, R. J. H., Rawnsley, K., and Sanderson, D. J. (2007). *Fractured reservoirs*. London, UK: Geological Society.

Long, J. C. S., Remer, J. S., Wilson, C. R., and Witherspoon, P. A. (1982). Porous media equivalents for networks of discontinuous fractures. *Water Resour. Res.* 18 (3), 645–658. doi:10.1029/wr018i003p00645

Long, J. C. S., and Witherspoon, P. A. (1985). The relationship of the degree of interconnection to permeability in fracture networks. *J. Geophys. Res.* 90 (B4), 3087. doi:10.1029/jb090ib04p03087

Ma, J., Yang, Y., Wang, H., Li, L., Wang, Z., and Li, D. (2018). How much CO2 is stored and verified through CCS/CCUS in China? *Energy Procedia* 154 (2018), 60–65. doi:10.1016/j.egypro.2018.11.011

Moinfar, A., Varavei, A., Sepehrnoori, K., and Johns, R. T. (2013). Development of an efficient embedded discrete fracture model for 3D compositional reservoir simulation in fractured reservoirs. *SPE J.* 19 (02), 289–303. doi:10.2118/154246-pa

Narr, W., Schechter, D. S., and Thompson, L. B. (2006). *Naturally fractured reservoir characterization*. Richardson, Texas: Society of Petroleum Engineers.

Nelson, R. A. (2001). *Geologic analysis of naturally fractured reservoirs*. Houston, Texas: Gulf Professional Publishing.

Nguyen, T. V., and Tran, X. V. (2016). Gas-assisted gravity drainage process for improved oil recovery in Bao Den fractured basement reservoir. *Sci. Tech. Dev. J.* 19 (1), 161–168. doi:10.32508/stdj.v19i1.514

Peng, Y., Zhao, J., Sepehrnoori, K., and Li, Z. (2020). Fractional model for simulating the viscoelastic behavior of artificial fracture in shale gas. *Eng. Fract. Mech.* 228, 106892. doi:10.1016/j.engfracmech.2020.106892

Schechter, D. (2002). Waterflooding and CO2 injection in the naturally fractured spraberry trend area. *J. Can. Petroleum Technol.* 41 (10), 10–15. doi:10.2118/02-10-das

Song, Z.-J., Li, M., Zhao, C., Yang, Y.-L., and Hou, J.-R. (2020). Gas injection for enhanced oil recovery in two-dimensional geology-based physical model of tahe fractured-vuggy carbonate reservoirs: Karst fault system. *Pet. Sci.* 17 (2), 419–433. doi:10.1007/s12182-020-00427-z

Vardon, D. R., Sherbacow, B. J., Guan, K., Heyne, J. S., and Abdullah, Z. (2022). Realizing 'net-zero-carbon' sustainable aviation fuel. *Joule* 6 (1), 16–21. doi:10.1016/j.joule.2021.12.013

Warren, J. E., and Root, P. J. (1963). The behavior of naturally fractured reservoirs. *Soc. Petroleum Eng. J.* 3 (03), 245–255. doi:10.2118/426-pa

Xu, F., Li, X., Gong, Y., Lei, C., Li, X., Yu, W., and Ding, Y. (2019). "A powerful and practical workflow for a naturally fractured reservoir with complex fracture geometries from modeling to simulation," in Proceedings of the SPE Paper URTEC-2019-1043-MS presented at the SPE/AAPG/SEG Unconventional Resources Technology Conference, Denver, Colorado, USA, July 2019, 22–24.

Xu F, F., Yu, W., Li, X., Miao, J., Zhao, G., Sepehrnoori, K., and Wen, G. (2018), "A fast EDFM method for production simulation of complex fractures in naturally fractured reservoirs," in Proceedings of the SPE Paper SPE-191800-18ERM-MS presented at the SPE/AAPG Eastern Regional Meeting, Pittsburgh, PA, USA, October 2018, 7–11.

Xu, Y., Cavalcante Filho, J. S. A., Yu, W., and Sepehrnoori, K. (2017). Discrete-fracture modeling of complex hydraulic-fracture geometries in reservoir simulators. *SPE Reserv. Eval. Eng.* 20 (02), 403–422. doi:10.2118/183647-pa

Zhou, W., Banerjee, R., Poe, B. D., Spath, J., and Thambynayagam, M. (2013). Semianalytical production simulation of complex hydraulic-fracture networks. *Soc. Petroleum Eng. J.* 19 (01), 06–18. doi:10.2118/157367-pa